The effect of barium titanate ceramic loading on the stress relaxation behaviour of barium titanate - silicone elastomer composites

Eshwar Reddy Cholleti[1], Jonathan Stringer[1], Piaras Kelly[2], Chris Bowen[3] and Kean Aw[1] *

1 Department of Mechanical Engineering, University of Auckland, 1010 Auckland, New Zealand; echo896@aucklanduni.ac.nz (E.R.C.); j.stringer@auckland.ac.nz (J.S.)
2 Department of Engineering Science, University of Auckland, 1010 Auckland, New Zealand; pa.kelly@auckland.ac.nz (P.K)
3 Department of Mechanical Engineering, University of Bath, BA2 7AY Bath, UK; c.r.bowen@bath.ac.uk
* Correspondence: k.aw@auckland.ac.nz; Tel.: +64-9-923-9767

Abstract

The stress relaxation behaviour of barium titanate (BTO) - elastomer (Ecoflex) composites used in a large strain sensor is studied using a generalized Maxwell-Wiechert model. In this paper, we examine the stress relaxation behaviour of ceramic polymer composites, by conducting stress relaxation tests on samples prepared with varying the particle loading by 0, 10, 20, 30 and 40 wt% of 100 nm or 200 nm BTO ceramic particles embedded in a Ecoflex silicone based hyperelastic elastomer. The influence of BTO on spring-dashpot coefficients of the Maxwell-Wiechert model is studied through the stress relaxation experiments. While a pristine Ecoflex silicone is predominantly a hyperelastic material, the addition of BTO made the composite behave as a visco-hyperelastic material. However, this behaviour has negligible effect on the electrical performance of the large strain sensor.

Keywords: Stress relaxation, Barium Titanate, Ecoflex, Visco-Hyper elastic, generalized Maxwell-Wiechert model.

INTRODUCTION

Recently, flexible and stretchable sensors have played a key role in a variety of applications such as, robotics, electronic skins, diagnostic devices and medical monitoring [1-5]. Strain sensors are a predominant member of the flexible sensor family, which require both stretchability and reversibility [6, 7]; examples of such sensors include Ecoflex and other soft silicones which are suitable for ultra-soft and skin-mountable strain sensors [8-10]. To increase the permittivity, and capacitance, of the Ecoflex silicone elastomer, barium titanate (BTO) ceramic nanoparticles are added. This enables the BTO-Ecoflex composite to be used as a sensitive capacitive strain sensor [11, 12]. The distribution and interaction between the ceramic filler and polymer matrix depends upon the particle size, surface area, and method of mixing to achieve uniform dispersion of the ceramic in polymer to avoid agglomeration [13].

Although, the effect of BTO particles in Ecoflex on the static mechanical properties, such as modulus and strength is understood to some extent [14], the possibly significant changes in the viscoelastic properties of BTO-Ecoflex composite have not as yet been explored. These characteristics can be important in load bearing applications where components are subjected to dynamic loading, as there is a potential for stress- or creep-relaxation. The pristine (filler-free) Ecoflex material is a silicone elastomer that has been tested and modelled by several researchers, who have demonstrated that it exhibits predominantly hyperelastic behaviour; which is implies the material can be subject to a large deformation without significant internal

energy dissipation [15-19]. In this research we have studied and explored the viscous nature in addition to this hyperelastic behaviour, brought about by the addition of BTO filler partcles to the Ecoflex by conducting stress relaxation experiments.

The Ecoflex silicone polymer is one of the electroactive polymers with Si-O bonds, which increases the dielectric constant (ε = X) [20] in comparison with other non-polar organic polymers, such as polytetrafluoroethylene (ε = 1.9) [21]. The dielectric constant of BTO-Ecoflex increases with increase in BTO filler loading and this increases the capacitance of the the sensing element when used in a capacitive strain sensor [11, 12]. In this work, 100 nm and 200 nm BTO partciles were selected due to their of their high dielectric constant (ε = X) [22, 23], and they have been used in the fabrication of highly stretchable inter digital capacitive (IDC) sensor. Fig.1 shows the testing facility for evaluating the capacitive sensors, where the change in capacitance with strain is measured.

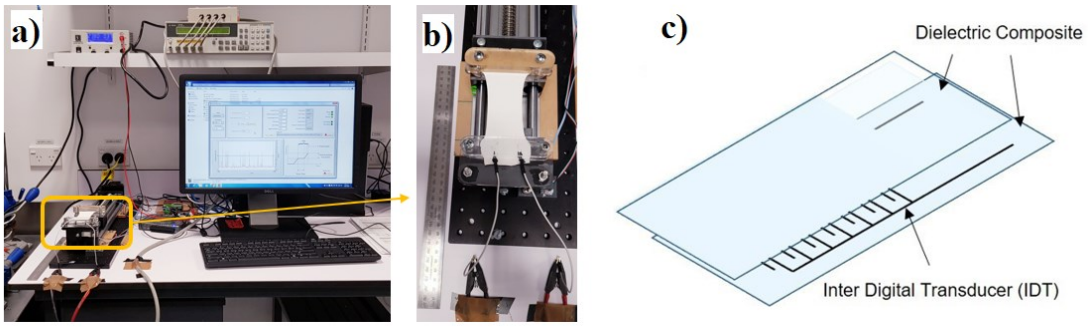

Fig.1. a) Testing of a highly stretchable capacitive sensor usage a testing rig showing an Agilent 4263B LCR meter b) The sensor being stretched by the motorized stage c) Schematic of the construction of a sensor [11, 12].

The visco-hyperelastic behaviour of BTO-Ecoflex composite can be studied by performing standard viscoelastic testing procedures, for example stress relaxation tests, creep recovery tests and strain-rate dependent loading or cyclic loading tests. In this paper we studied the effect of BTO loading on the visco-hyperelastic behaviour of BTO-Ecoflex composite by conducting stress relaxation tests. In a stress relaxation experiment, a constant strain is applied, and continued decrease in stress is needed to maintain a given deformation or loss of stiffness with time is measured. The measured relaxation time indicates how fast the stress decays after an initial deformation. When a stress relaxation experiment is performed, ideal viscous materials begin to relax instantaneously, whereas ideal elastic materials do not undergo any relaxation. Viscoelastic solids, that lie between these two extremes, relax gradually and eventually reach a non-zero equilibrium stress, whereas the residual stress for visco-elastic fluids is zero.

Several researchers have studied the viscoelastic characteristics of polymers and polymer composites, Examples include Bipul Barua *et al*, who modelled the stress relaxation behaviour of thermosetting polyurethane solid and foams using a Generalized Maxwell-Wiechert (GMW) model [24]. Julie Diani *et al*, modelled the non-linear visco-hyperelastic behaviour of EPDM (ethylene propylene diene) elastomer filled with carbon black by using the GMW model [25]. Dong Yun Choi *et al*, developed a simple model to describe the relationship between the viscoelasticity of an elastomer (Ecoflex 00-50) and the hysteresis of electrical response of the strain sensor consisting of a stretchable serpentine channel by using the second order GMW model [26]. Gexin You *et al*, used the GMW model to predict the stress relaxation moduli of

polyurethane fiber composite [27]. T.Cui *et al*, studied the stress relaxation behaviour of liquid silicone rubber by using GMW model [28]. Therefore, the majority of researchers have used a GMW model or a modified GMW model to study the viscoelastic properties of polymer composites from literature [15-19, 24-32]. In this study, from literature and preliminary curve fitting of the experimental stress relaxation data, we found the Generalized Maxwell-Wiechert model (Prony-series) is the most suitable model to study the influence of BTO loading on visco-hyperelastic behaviour of a BTO-Ecoflex composite material, and this is no explained in detail within in following sections.

EXPERIMENTS

MATERIALS AND METHODS

Test samples were prepared using BTO ceramic powder, from TPL Inc (Albuquerque, USA), and Ecoflex^{TM} 00-30 from Smooth-On (USA). BTO ceramic powder particles of size 100 nm and 200 nm were used in this work. Three samples for each composition was prepared for the stress relaxation experiments, namely 0 wt% (pristine Ecoflex), 10 wt%, 20 wt%, 30 wt% and 40 wt% of 100 nm and 200 nm BTO. The samples were prepared by adding BTO ceramic powder of the required wt% into Ecoflex^{TM} 00-30 in the liquid state. The composite was then mixed using a planetary mixture (Mazerustar KK-50S). The mixture was then poured into an acrylic mold (Fig.2) and left to cure at room temperature for a minimum of 12 hrs. Sample dimensions were 150 mm length, 50 mm width and 2 mm thickness, and are as shown in the Fig.2.

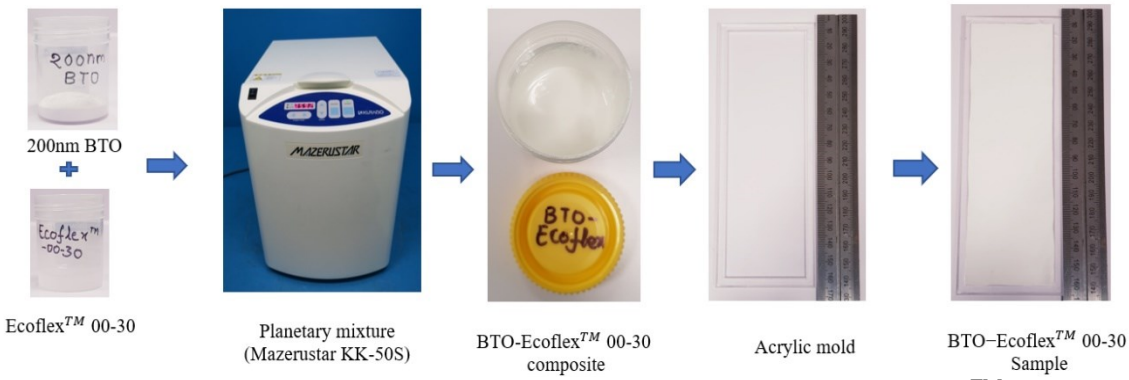

Fig.2. Sample preparation process of 40 wt% 200 nm BTO-Ecoflex^{TM} 00-30.

TEST SETUP

The most extensively used method to study and compare viscoelastic compounds properties is the stress relaxation test. The stress relaxation experiment is performed using an Instron 5567 testing machine. As in a tensile test, the effective length of the sample is defined as the distance between the two holders, which is fixed at 100 mm length, then fed the instrument by input data such as thickness, width of the sample and strain rate. The crosshead is then moved to apply a tensile strain to the sample by 100% (effectively doubling the length) at a rate of 500 mm/min and held at 100% strain for 60 minutes on extension control to monitor the slow decay of stress. The decrease in stress was recorded by using 50 N load cell, as seen in Fig.3.a. The period of recording the data were continued for 60 minutes and the values taken were used for drawing the relationship between time and stress. The test samples are marked with dots to represent the gauge length of 50 mm and gauge width of 20 mm, see Fig.3.b. The same

procedure was used for each sample of different compositions used in the study. All experiments were performed at room temperature.

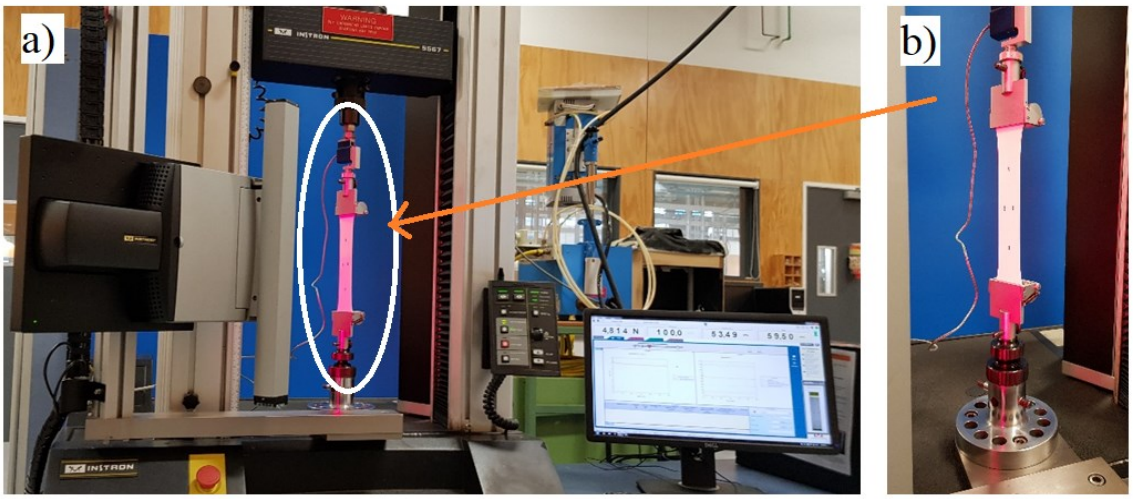

Fig.3.a). Instron 5567 load frame with Interface SM-50 N SN: 625735 load cell and video recording setup. b). Test sample marked with dots to represent the gauge length and gauge width.

RESULTS AND DISCUSSION

GENERALIZED MAXWELL-WIECHERT MODEL

One of the elemental rheological viscoelastic models that can be used to predict relaxation behaviour is the Maxwell model, which consists of a viscous Newtonian damper and an elastic Hookean spring in series. The total strain equals the summation of the strains in the elastic and viscous elements. When a displacement is applied instantaneously, as in a relaxation test, the viscous element needs a finite time to respond, whereas the spring displaces instantaneously. At time zero, the initial total displacement is that of the spring. As time proceeds, the displacement in the spring decreases, but increases in the damper. After an infinite time, the strain in the elastic part is zero (and so the stress is zero). However, this behaviour is not seen in most real elastomers, that is, the stress in these materials does not decay to zero. For this reason, models incorporating multiple springs and dashpots are needed, a generic example being the *generalised Maxwell model* [33].

The generalized Maxwell model, is composed of springs (representing ideal solids, they account for the pure hyperelastic or elastic behaviour of viscoelastic materials) and dashpots (representing ideal fluids, they account for the viscous behaviour of visco-hyper elastic or viscoelastic materials). A combination of a number of Maxwell elements arranged in a parallel configuration, is the most general form of the linear model that is used to describe the stress relaxation behaviour of hyperelastic [29], viscoelastic [32] or visco-hyper elastic [25, 31] materials. Based on the nature of material chosen, the behaviour of the springs is considered either elastic or hyperelastic [25, 29-32]. The simple Maxwell model consisting of a dashpot in series with a hyperelastic spring has a single relaxation time constant, $\tau = \eta/E$ and, as mentioned, real polymers do not relax with a single relaxation time because the longer molecular segments takes more time to relax than the shorter molecular segments, this contributes the combination of various relaxation times, which is not able to explained by single

Maxwell element alone [25, 29-32], therefore multiple spring-dashpots Maxwell elements are necessary to accurately represent the relaxation of a real material.

To model the pure elastic response of real materials that gradually reach an equilibrium (non-zero stress) elastic state during a relaxation test, an additional spring with an elastic equilibrium modulus can be added in parallel to the generalized Maxwell model. In this way, the generalized Maxwell model is transformed into the generalized Maxwell-Wiechert model (GMW model) [25, 29-32]. In the general case, the GMW model consists of a spring of elastic modulus $\boldsymbol{E_\infty}$ in parallel with $\boldsymbol{n}$ Maxwell elements, with the $\boldsymbol{n^{th}}$ Maxwell element having a time constant $\boldsymbol{\tau_n}$ and a spring of elastic modulus $\boldsymbol{E_n}$. Since all of the elements are connected in parallel, they will all have the same strain $\varepsilon(t)$ at a time t during a relaxation test, and the overall stress σ transmitted by the GMW model is the stress in the isolated spring plus that in each of the Maxwell spring-dashpot arms, see Fig.4.a.

The accuracy of the description of the relaxation behaviour of real materials depends upon the order of the Maxwell elements. The use of higher order Maxwell elements will increase the complexity of the model, and this will be a challenging task to find number of material parameters. However, numerical experiments with different numbers of elements, using the *cftool* feature in MATLAB, showed that the second order GMW model shown in the Fig.4.b was suitable to fit the relaxation experimental data of BTO-Ecoflex composite material.

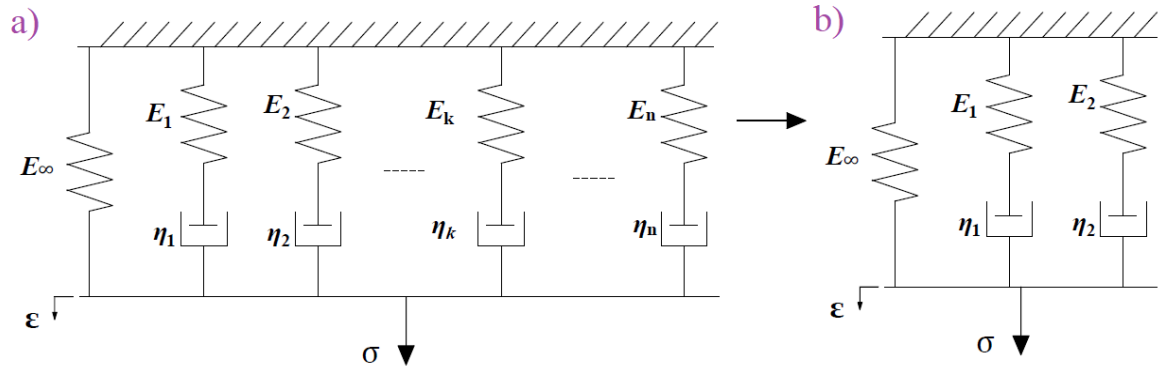

Fig.4.a). Generalized Maxwell-Wiechert model b). Generalized Maxwell-Wiechert branches suitable for BTO-Ecoflex visco-hyperelastic composite material.

The response in each Maxwell element of the GMW model is given by [32]

$$\dot{\varepsilon_k} = \frac{\dot{\sigma_k}}{E_k} + \frac{\sigma_k}{\eta_k} \quad , \mathrm{k} = 1 \, , 2 \, , \ldots..\mathrm{n} \qquad (1)$$

where E_k is the elastic modulus, and h_k is the viscosity of the k^{th} element. If a constant strain ε_0 is imposed at t = 0, the solution of Eq.1 is given by

$$\sigma_k(t) = \sigma_{k,0}\, e^{-t/\tau_k} \quad , \quad \tau_k = \frac{\eta_k}{E_k} \qquad (2)$$

where $\sigma_{k,0}$ $(= E_k \varepsilon_0)$ is the initial stress at t = 0, and τ_k is the relaxation time of the k^{th} element. Then the total stress is given by

$$\sigma(t) = E_\infty \varepsilon_0 + \sum_{k=1}^{n} \sigma_{k,0}\, e^{-\frac{t}{\tau_k}}$$

$$= \varepsilon_0 \left(E_\infty + \sum_{k=1}^{n} E_k e^{-\frac{t}{\tau_k}} \right) \qquad (3)$$

The relaxation modulus $E(t)$ is defined as

$$E(t) = \frac{\sigma(t)}{\varepsilon_0} = E_\infty + \sum_{k=1}^{n} E_k\, e^{-\frac{t}{\tau_k}} \qquad (4)$$

which is essentially the Prony series representation. Here, $\boldsymbol{E}_\infty$ $(= \lim_{t\to\infty} E(t))$ is the final (or equilibrium) modulus, and $E_0 = E_\infty + \sum_{k=1}^{n} E_k$ is the instantaneous modulus. A pair of E_k and τ_k is referred to as a Prony pair.

To study the stress relaxation behaviour of the BTO-Ecoflex composite material, we have undertaken preliminary curve fitting of stress relaxation experimental data with basic Maxwell model and first, second and third order of GMW models using the *cftool* feature in MATLAB, such that we found the second order GMW model is the most suitable model, that fits with the experimental stress relaxation test data. The second order with GMW model is stated as follows,

$$E(t) = E_\infty + \sum_{i=1}^{2} E_i e^{-t/\tau_i} \qquad (5)$$

$$E(t) = E_\infty + E_1 e^{-tE_1/\eta_1} + E_2 e^{-tE_2/\eta_2} \qquad (6)$$

Here, E_∞ is the equilibrium modulus of the sample when it has fully relaxed; E_1, E_2 and τ_1, τ_2 are Prony parameter and relaxation time, respectively.

SPRING-DASHPOTS COEFFICIENTS (PRONY SERIES) OBTAINED BY CURVE FITTING GMW MODEL USING MATLAB

Initially, we have taken the stress relaxation data from Instron 5567 (Fig.3.a) of the 40 wt% 200 nm BTO-Ecoflex composite samples, as seen in Fig.2 The curve fitting of the 40 wt% 200 nm BTO-Ecoflex composite sample stress relaxation data is performed in MATLAB with *cftool* feature, using Eq.6, in order to find out the Prony parameters and equilibrium modulus. The Prony parameters and equilibrium modulus are found for three samples (max, min and average) of each composition i.e 0 wt%, 10 wt%, 20 wt%, 30 wt% and 40 wt% of 200 nm and 100 nm BTO-Ecoflex, the curve fitting of the second order GMW model with the experimental data is presented in Fig. 5, 6 and 7.

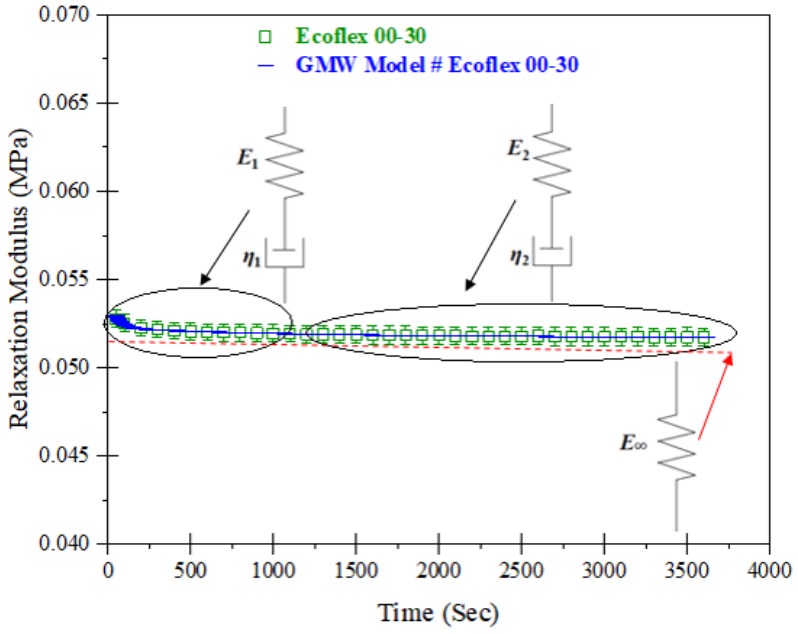

Fig.5. Stress relaxation of pristine Ecoflex (0 wt% BTO) curve fitting with GMW model.

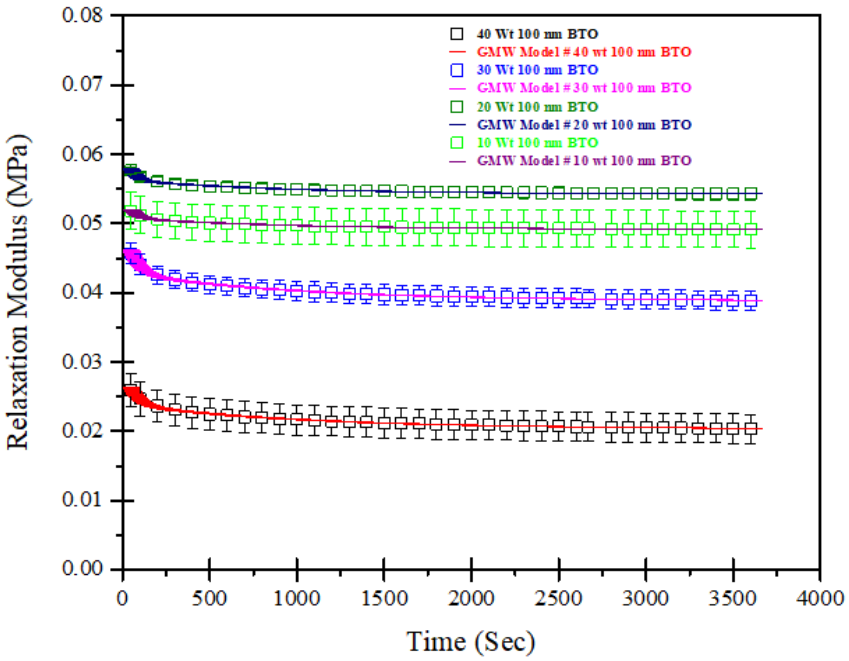

Fig.6. Stress relaxation of 40, 30, 20, 10 wt% 100 nm BTO-Ecoflex composite curve fitting with GMW model.

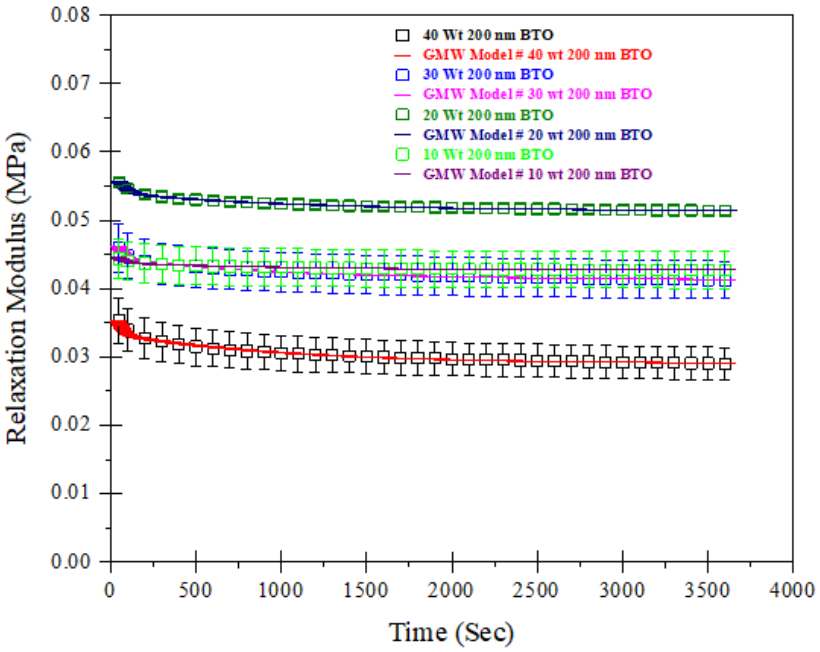

Fig.7. Stress relaxation of 40, 30, 20, 10 wt% 200 nm BTO-Ecoflex composite curve fitting with GMW model.

The study of the mechanical behaviour of BTO-Ecoflex composite indicates that an increase in wt% of BTO in Ecoflex of more than 5 wt%, leads to a decrease in the stiffness of the BTO-Ecoflex composite due to agglomeration of the BTO powder in the Ecoflex polymer [14]. The following stress relaxation study is performed on the BTO-Ecoflex to know the viscoelastic characters of BTO-Ecoflex composite.

The relaxation modulus decreased with increase in wt% of BTO (100 nm and 200 nm). In addition, the range of decrease of stress relaxation increased, with increase in wt% of BTO (100 nm and 200 nm) this indicates a greater viscoelastic response of BTO-Ecoflex composite, as seen by comparing Fig.5 to Fig.7.

RELATIONSHIP BETWEEN THE SPRING-DASHPOT COEFFICIENTS (PRONY SERIES) OF 100 NM AND 200 NM BTO-ECOFLEX COMPOSITES

The relaxation response of BTO-Ecoflex composite follows the second order GMW model from the Fig.5, 6 and 7. This indicates that the BTO-Ecoflex composite exhibits a visco-hyperelastic nature. The relaxation function of polymers and polymer composites is majorly modelled with a Prony series from literature. The effect on the material coefficients (Prony series) of BTO-Ecoflex composites by wt% of BTO is studied by plotting the materials coefficient data with filler content, as presented in the Fig.8 to Fig.12.

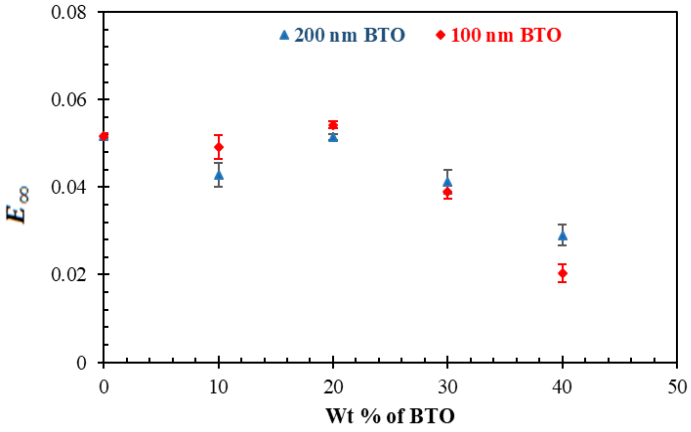

Fig.8. The hyperelastic residual spring coefficient E_∞ varies with wt% of BTO

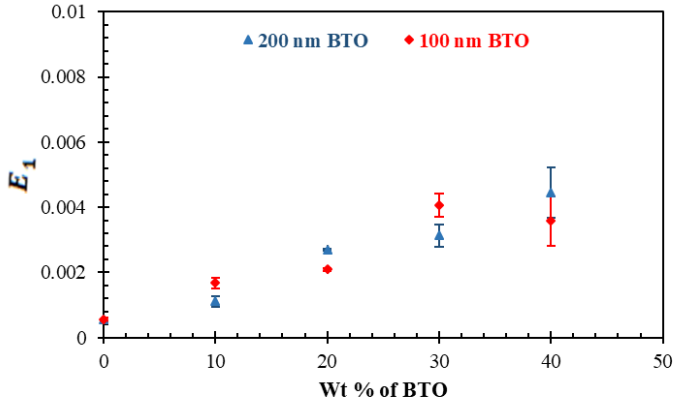

Fig.9. The hyperelastic spring coefficient E_1 varies with wt% of BTO

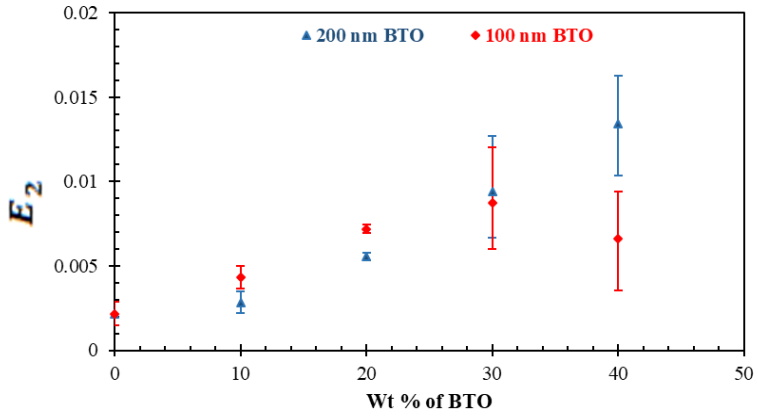

Fig.10. The hyperelastic spring coefficient E_2 varies with wt% of BTO

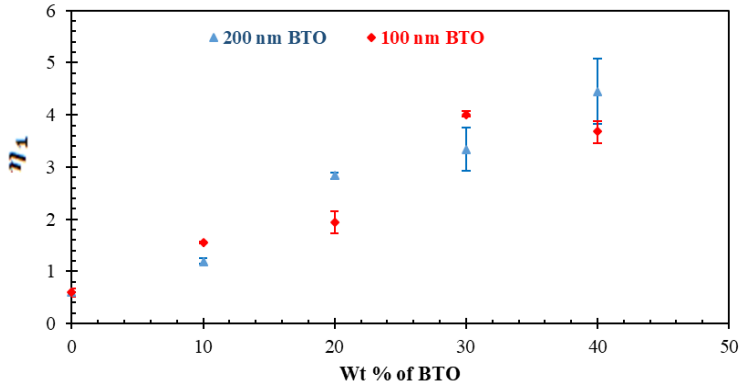

Fig.11. The viscous dashpot coefficient η_1 varies with wt% of BTO

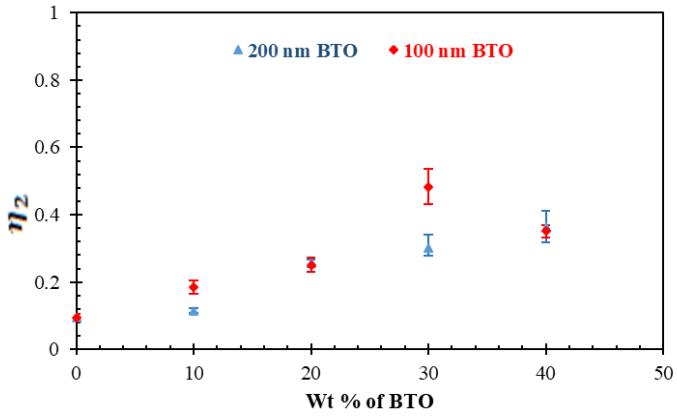

Fig.12. The viscous dashpot coefficient η_2 varies with wt% of BTO

The maximum, average and minimum values of the coefficients of different BTO loading into Ecoflex is plotted in the Fig.8 to Fig.12. It is clear that the elastic moduli (E_1, E_2) and viscosity coefficients (η_1, η_2) increases with the BTO loading (Fig.9 to Fig.12). However, there is a smaller effect on the change in η_2 with an increase in BTO loading. In contrast, there is an overall decrease in equilibrium modulus (E_∞) with the increase in the wt% of BTO, as observed Fig.8. Overall, a similar materials coefficient trend is observed between the 100 nm BTO-Ecoflex and 200 nm BTO-Ecoflex composite materials, such that the 100 nm and 200 nm BTO-Ecoflex composites shows no considerable difference in their visco-hyperelastic nature.

[describe how error bars are determined]

OUTPUT SIGNAL OF INTERDIGITAL CAPACITIVE STRAIN SENSOR SUBJECTED TO STRESS RELAXATION

To evaluate the materials as a capactivie sensor, stretchable IDC sensors fabricated with 0 wt% (pristine Ecoflex), 40 wt% of 100 nm and 200 nm BTO-Ecoflex, are subjected to stress relaxation for 1hr respectively. The IDC sensor is fixed to the motorized moving stage as shown in Fig.1.b, then the IDC is subjected to 100 % strain at the rate of 420 mm/min. The change in capacitance of IDC with respective substrates are plotted in the Fig.13. The testing is performed at room temperature by using the motorized moving stage as shown in Fig.1(a).

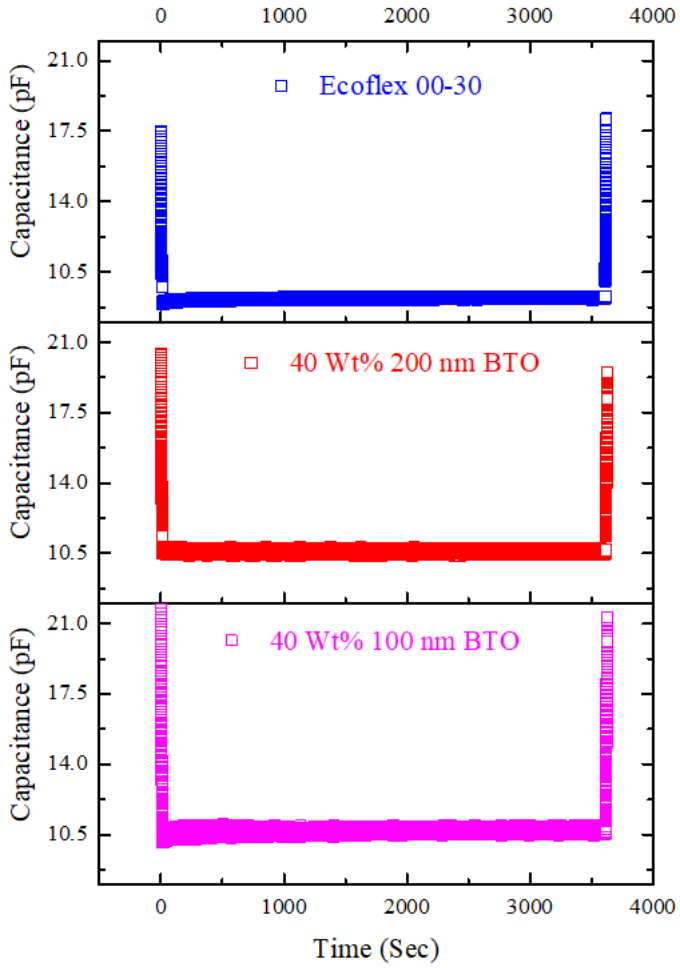

Fig.13. Capacitance of IDC with 0 wt% (pristine Ecoflex), 40 wt% of 100 nm and 200 nm BTO-Ecoflex substrates.

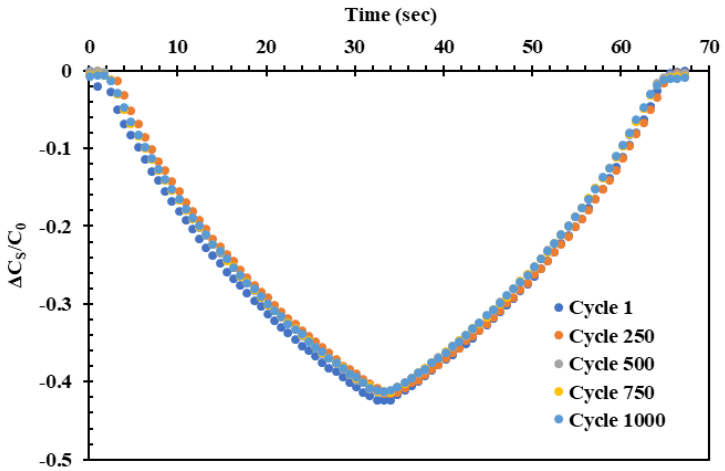

Fig.14. Relative change in capacitance ($\Delta C_S/C_0$) versus time of the IDC sensor with 40 wt% 200 nm BTO-Ecoflex composite substrate is stretched to 100% for 1000 cycles [12].

Despite the relaxation time response of the BTO-Ecoflex substrates made from 40 wt% 100 nm and 200 nm BTO-Ecoflex composite, the capacitive output of the stretchable IDC sensors remains stable when remain stretched at 100% strain over 1hr period. The capacitive outputs of the IDC sensors return to the initial capacitance value almost immediately when relaxed. Despite the BTO-Ecoflex composite exhibits stress relaxation behaviour, the capacitance of the IDC sensor remains almost constant during this period.

In addition, the capacitance of the IDC sensor with a Ecoflex substrate with 40 wt% of 200 nm BTO remains unchanged even after being subjected to 1000 stretch/relax cycles as shown in Fig.14 [12]. This demonstrates that the visco-hyperelastic behaviour of the BTO-Ecoflex composite substrate has no significant effect on the capacitance of IDC sensor.

CONCLUSION

In this study a series of stress relaxation experiments were performed to characterize the time dependent visco-hyperelastic behaviour of BTO-Ecoflex composite. The second order GMW model is used to curve fit the stress relaxation behaviour of BTO-Ecoflex composite by using *cftool* feature in MATLAB, in order to determine the Prony pairs (material coefficients). The increase in BTO loading in Ecoflex, acts to increase the spring and viscous dashpot coefficients (Prony series). However, the residual spring coefficient decreases with an increase in the BTO loading. The stress relaxation experiments performed on the IDC strain sensors with BTO-Ecoflex substrate show that the output capacitance is not affected by the stress relaxation behaviour even 1000 stretch/relax cycles. In conclusion, the addition of BTO into Ecoflex resulted in a viscous-hyperelastic material, but this has no effect on the electrical performance of the IDC large strain sensor. Hence, this provides important data of ensuring the reliability of large strain capacitive sensor materials.

REFERENCE LIST

1. Cabibihan, J.J. and M.C. Carrozza, *Influence of the Skin Thickness on Tactile Shape Discrimination.* 2012 4th Ieee Ras & Embs International Conference on Biomedical Robotics and Biomechatronics (Biorob), 2012: p. 1681-1685.
2. Wang, H.B., et al., *Design and Characterization of Tri-Axis Soft Inductive Tactile Sensors.* Ieee Sensors Journal, 2018. **18**(19): p. 7793-7801.
3. Berselli, G., et al., *Engineering Design of Fluid-Filled Soft Covers for Robotic Contact Interfaces: Guidelines, Nonlinear Modeling, and Experimental Validation.* Ieee Transactions on Robotics, 2011. **27**(3): p. 436-449.
4. Elango, N. and A.A.M. Faudzi, *A review article: investigations on soft materials for soft robot manipulations.* International Journal of Advanced Manufacturing Technology, 2015. **80**(5-8): p. 1027-1037.
5. Amjadi, M., et al., *Stretchable, Skin-Mountable, and Wearable Strain Sensors and Their Potential Applications: A Review.* Advanced Functional Materials, 2016. **26**(11): p. 1678-1698.
6. Gu, J., et al., *Wearable Strain Sensors Using Light Transmittance Change of Carbon Nanotube-Embedded Elastomers with Microcracks.* Acs Applied Materials & Interfaces, 2020. **12**(9): p. 10908-10917.

7. Xia, Y., et al., *Practical and Durable Flexible Strain Sensors Based on Conductive Carbon Black and Silicone Blends for Large Scale Motion Monitoring Applications.* Sensors, 2019. **19**(20).
8. Guo, X.H., et al., *Highly stretchable strain sensor based on SWCNTs/CB synergistic conductive network for wearable human-activity monitoring and recognition.* Smart Materials and Structures, 2017. **26**(9).
9. Chen, J.W., et al., *An overview of stretchable strain sensors from conductive polymer nanocomposites.* Journal of Materials Chemistry C, 2019. **7**(38): p. 11710-11730.
10. Amjadi, M., Y.J. Yoon, and I. Park, *Ultra-stretchable and skin-mountable strain sensors using carbon nanotubes-Ecoflex nanocomposites.* Nanotechnology, 2015. **26**(37).
11. Cholleti, E.R., et al. *Barium Titanate Elastomer composite based capacitive stretch sensor*. in *2019 IEEE/ASME International Conference on Advanced Intelligent Mechatronics (AIM)*. 2019.
12. Cholleti, E.R., et al., *Highly Stretchable Capacitive Sensor with Printed Carbon Black Electrodes on Barium Titanate Elastomer Composite.* Sensors, 2019. **19**(1).
13. Ziegmann, A. and D.W. Schubert, *Influence of the particle size and the filling degree of barium titanate filled silicone elastomers used as potential dielectric elastomers on the mechanical properties and the crosslinking density.* Materials Today Communications, 2018. **14**: p. 90-98.
14. Kumar, A., D. Ahmad, and K. Patra, *Barium titanate particle filled silicone elastomer composite: Preparation and evaluation of morphology and mechanical behaviour.* Journal of Physics: Conference Series, 2019. **1240**: p. 012049.
15. Piovarci, M., et al., *An Interaction-Aware, Perceptual Model for Non-Linear Elastic Objects.* Acm Transactions on Graphics, 2016. **35**(4).
16. Steck, D., et al., *Mechanical responses of Ecoflex silicone rubber: Compressible and incompressible behaviors.* Journal of Applied Polymer Science, 2019. **136**(5).
17. Zhang, L., et al., *Synthesis of percolative hyperelastic conducting composite and demonstrations of application in wearable strain sensors.* Materials Letters, 2018. **233**: p. 306-309.
18. Chen, L.S., et al., *Design and modeling of a soft robotic surface with hyperelastic material.* Mechanism and Machine Theory, 2018. **130**: p. 109-122.
19. Pineda, F., et al., *Using electrofluidic devices as hyper-elastic strain sensors: Experimental and theoretical analysis.* Microelectronic Engineering, 2015. **144**: p. 27-31.
20. Eom, S. and S. Lim, *Stretchable Complementary Split Ring Resonator (CSRR)-Based Radio Frequency (RF) Sensor for Strain Direction and Level Detection.* Sensors, 2016. **16**(10).
21. Barber, P., et al., *Polymer Composite and Nanocomposite Dielectric Materials for Pulse Power Energy Storage.* Materials, 2009. **2**(4): p. 1697-1733.
22. Zheng, P., et al., *Grain-size effects on dielectric and piezoelectric properties of poled BaTiO3 ceramics.* Acta Materialia, 2012. **60**(13-14): p. 5022-5030.
23. Wada, S., et al., *Size dependence of dielectric properties for nm-sized barium titanate crystallites and its origin.* Journal of the Korean Physical Society, 2005. **46**(1): p. 303-307.
24. Barua, B. and M.C. Saha, *Tensile Stress Relaxation Behavior of Thermosetting Polyurethane Solid and Foams: Experiment and Model Prediction.* Journal of Engineering Materials and Technology-Transactions of the Asme, 2011. **133**(4).

25. Diani, J., M. Brieu, and P. Gilormini, *Observation and modeling of the anisotropic visco-hyperelastic behavior of a rubberlike material.* International Journal of Solids and Structures, 2006. **43**(10): p. 3044-3056.
26. Choi, D.Y., et al., *Highly Stretchable, Hysteresis-Free Ionic Liquid-Based Strain Sensor for Precise Human Motion Monitoring.* ACS Appl Mater Interfaces, 2017. **9**(2): p. 1770-1780.
27. You, G.X., et al., *Model and prediction of stress relaxation of polyurethane fiber.* Materials Research Express, 2018. **5**(3).
28. Cui, T., et al., *Service life estimation of liquid silicone rubber seals in polymer electrolyte membrane fuel cell environment.* Journal of Power Sources, 2011. **196**(3): p. 1216-1221.
29. Bodai, G. and T. Goda, *A New, Tensile Test-based Parameter Identification Method for Large-Strain Generalized Maxwell-Model.* Acta Polytechnica Hungarica, 2011. **8**(5): p. 89-108.
30. Yildiz, O., et al., *Pasting properties, texture profile and stress-relaxation behavior of wheat starch/dietary fiber systems.* Food Research International, 2013. **53**(1): p. 278-290.
31. Kraus, M.A., et al., *Parameter identification methods for visco- and hyperelastic material models.* Glass Structures & Engineering, 2017. **2**(2): p. 147-167.
32. Chae, S.H., et al., *Characterization of the Viscoelasticity of Molding Compounds in the Time Domain.* Journal of Electronic Materials, 2010. **39**(4): p. 419-425.
33. Ayoub, G., et al., *Modeling the low-cycle fatigue behavior of visco-hyperelastic elastomeric materials using a new network alteration theory: Application to styrene-butadiene rubber.* Journal of the Mechanics and Physics of Solids, 2011. **59**(2): p. 473-495.